Iranian Journal of Microbiology
Volume 16 Number 3 (June 2024) 376-388

ORIGINAL ARTICLE

Effect of collagen hydrogel containing *Lavandula officinalis* essential oil nanoemulsion in wound healing of infectious burn

Hossein Teymouri[1], Mojgan Mohammadimehr[1,2*], Mohammad Ahanjan[3], Somayeh Sheidaei[4], Majid Saeedi[5], Amir Mellati[6]

[1]Infectious Diseases Research Center, Aja University of Medical Sciences, Tehran, Iran
[2]Department of Laboratory Sciences, Faculty of Para Medicine, Aja University of Medical Sciences, Tehran, Iran
[3]Department of Medical Bacteriology and Virology, Faculty of Medicine, Mazandaran University of Medical Sciences, Sari, Iran
[4]Department of Pathology, School of Medicine, Mazandaran University of Medical Sciences, Sari, Iran
[5]Department of Pharmaceutics, School of Pharmacy, Mazandaran University of Medical Sciences, Sari, Iran
[6]Department of Tissue Engineering and Regenerative Medicine, School of Advanced Technologies in Medicine, Mazandaran University of Medical Sciences, Sari, Iran

Received: January 2024**, Accepted:** April 2024

ABSTRACT

Background and Objectives: The main cause of mortality in burn patients is infection from burns. Drug-resistant bacteria are the main causes of wound infection, so alternative antibiotic therapies hold significant importance. The objective of this study was to examine the impact of a collagen hydrogel that contains a nanoemulsion of *Lavandula* essential oil on the healing process of infected burn wounds.

Materials and Methods: In this experimental study, 20 rats were randomly divided after applying burns with a 10 mm diameter hot plate and infecting the wounds with multidrug-resistant *Pseudomonas aeruginosa* into four groups, including a positive control, a negative control, the first experiment (collagen hydrogel), and the second experiment (collagen hydrogel containing *Lavandula* essential oil nanoemulsion). On the 4th, 11th, and 18th days, tissue samples were taken for pathology studies. The important parameters in burn wound healing with hematoxylin and eosin and Masson's trichrome staining methods were investigated and scored according to Abramov's method.

Results: Based on the pathology findings, experimental groups 1 and 2 compared to the negative and positive control groups were effective in rat infection wound healing. The hydrogel scaffold in the experimental groups increased fibroblasts and angiogenesis compared to the control groups. Epithelization was noticed only in the hydrogel group containing nanoemulsion.

Conclusion: The study findings suggest that the use of collagen hydrogel with *Lavandula* essential oil nanoemulsion has potential as a wound dressing. This is because it has the potential to effectively promote healing and act as an antibacterial agent to prevent infections.

Keywords: *Lavandula*; Wound healing; Collagen; Hydrogels; Burns

*Corresponding author: Mojgan Mohammadimehr, Ph.D, Infectious Diseases Research Center, Aja University of Medical Sciences, Tehran, Iran; Department of Laboratory Sciences, Faculty of Para Medicine, Aja University of Medical Sciences, Tehran, Iran. Tel: +98-21-49822995 Fax: +98-21-43822992 Email: mojganmehr20@yahoo.com

INTRODUCTION

More than 265,000 cases of burn injuries result in fatalities each year. Burn wound infection not only increases the death rate among hospitalized patients but also delays the healing process. The primary therapeutic approaches for treating burn wounds involve the use of artificial dermal replacements and dressing care. The use of common antibiotics has declined due to the persistent rise of multidrug-resistant (MDR) microorganisms (1). Handling wound burn infections caused by MDR bacteria will surely lead to improved healthcare on a global level. The rise of multidrug-resistant Gram-negative bacteria poses a significant threat to the effectiveness of therapies in both industrialized and poor countries. *Pseudomonas aeruginosa*, for instance, is a highly problematic bacteria that poses a global concern (2).

Flexible, biodegradable, and adequately gas-permeable wound dressing materials are necessary to reduce the rate of infection (3). The capacity to stick and having control over how much exudate a wound can absorb are important additional factors. Traditional dressings, however, are typically arid and difficult to use (4). Natural biopolymers are utilized as wound dressings due to their biocompatibility, biodegradability, and resemblance to the extracellular matrix (ECM), which allows cell attachment due to their microporous structure (5).

Hydrogels are polymer networks that have a three-dimensional structure and are hydrophilic, allowing them to absorb large amounts of liquid. These compounds can absorb several times the polymer's weight of water without disintegrating. Hydrogels have a flexible and elastic nature, exhibiting physical and chemical characteristics that closely resemble those of biological tissues. Hydrogels are biocompatible, controlled, biodegradable, and hydrating for burn wounds, but they can also transport drugs. Hydrogels absorb wound exudate better than other dressing materials (6). Collagen is a protein that maintains the structural integrity of cells and tissues. Myofibroblasts and fibroblasts produce collagen in the skin. Collagen is arranged in the form of fibrils and is constantly exposed to tension and shear forces in the skin, tendons, and bones. This protein exhibits low immunogenicity, exceptional biocompatibility, and biodegradability and promotes cellular adhesion, proliferation, and growth. So it is an exceedingly appropriate choice for tissue engineering scaffolds (7).

Nanoemulsions (NEs) are a distinct approach to medication delivery that involves using carrier systems for the encapsulation of active substances. NEs possess a composition and structure that allow them to include a larger quantity of pharmacological content in comparison to other topical products, including ointments, creams, gels, and lotions. Eventually, the dispersed oil droplet phase of NEs can enhance the solubility of hydrophobic medicines with low water solubility. Due to the composition of NEs, the medicine will effectively penetrate the deeper skin layers;, more precisely, the stratum germinativum and dermis are the specific areas where wound healing and angiogenesis occur. This treatment can effectively promote collagen deposition and regenerate skin tissue. Nanoparticles' (NP) size allows them to enter the wound and engage target molecules, releasing drugs or bioactive substances locally and affecting healing. NEs are specifically engineered to effectively cure burn injuries and have been scientifically demonstrated to possess extensive antibacterial and antifungal characteristics. These emulsions chemically bond with the lipid layer of microbial outer membranes, causing the membranes to become unstable and resulting in the destruction of pathogens. Nanomaterials expedite the process of wound healing because of their high surface area-to-volume ratio and ability to provide medication (8-11).

Essential oils (EOs), recognized as volatile oils, represent highly complicated mixtures. These liquids are volatile, aromatic, and greasy. They are obtained from different parts of plants and are used in numerous industries. They have attracted considerable study because of their antibacterial, antifungal, anti-inflammatory, and antioxidant properties. They have attracted considerable attention and are a promising alternative to synthetic drugs (12, 13).

Lavandula officinalis essential oil (LEO) has been shown to accelerate wound contraction and exhibit antibacterial properties, making it a promising candidate for topical therapy (14, 15). According to the points mentioned about NEs, the effectiveness of EOs can be enhanced by incorporating them into an appropriate nanocarrier. The aim of this study was to study the effect of *lavandula* essential oil nanoemulsion (LEO-NE) loaded into a collagen hydrogel scaffold on the healing of burn wounds infected with MDR *P. aeruginosa* in an animal model. This investigation aimed to fill the need for research about the effects of LEO on *P. aeruginosa* infection wounds.

MATERIALS AND METHODS

Material selection. LEO was purchased from Barij Co. (Kashan, Iran). Tween 80 and Span 60 (Merck, Germany) were used. *P. aeruginosa*, isolated from a burn patient and used in this study. Antibiotic disks (Mast Group Co., UK) were used. 20 male Wistar rats (250-270 g) were obtained from the Animal Center of Mazandaran University of Medical Sciences (Mazandaran, Iran). This study was conducted in the Microbiology Department, Faculty of Medicine, Mazandaran University of Medical Sciences, Mazandaran, Iran.

Gas Chromatography/Mass Spectroscopy (GC/MS) analysis of the essential oil. The GC/MS analysis was conducted using a Hewlett-Packard 6890/5972 system equipped with a DB-5 capillary column measuring 30 m in length and 0.25 mm in diameter, with a film thickness of 0.25 μm. The samples were carried using helium as the carrier gas at a flow rate of 2 mL/min in the present investigation. 70 eV electron energy was employed for the execution of mass spectrometry. The mass scan range spanned from 40 to 400 m/z, with a sampling rate of 1.0 scans per second. Quantitative data were achieved by electronically integrating the FID peak areas. The constituents of the oil were discovered by utilizing the retention time, retention indices relative to C9-C28n-alkanes, and computer matching with the Wiley 275.L. library. The acquired mass spectra were compared to the actual samples and data documented in the literature (16). The percentage composition of EOs was determined by calculating the ratio of the peak area obtained from GC analysis without making any adjustments or corrections.

Preparation and analysis of LEO-NE. LEO-NE was created using the high-pressure homogenization technique for EOs. To prepare the LEO-NE (1% v/w) was dispersed in a lipophilic surfactant. (Span 60, 1% v/w). The EO (1% v/w) was distributed in a heated aqueous solution containing surfactant containing 2% v/w Tween 80. Then the homogenization of the mixture was performed by a high-shear homogenizer (D-91126 Schwabach, Heidolph, Germany) for 1 minute at 8000 rpm. The obtained pre-emulsion was homogenized using an APV Micron Lab 40 (APV Systems, Unna, Germany) at high pressure (3 cycles, 500 bar). The Z-average mean particle size, polydispersity index (PDI), and Zeta potential were determined using dynamic light scattering (DLS) with a Zetasizer Nano instrument manufactured by Malvern Instruments. The measurements were conducted at a temperature of 65 degrees Celsius and at an angle of 27 degrees (16).

Preparation of collagen/LEO-NE hydrogel. A solution of rat tail collagen was prepared by dissolving it in 1.8 mL of acetic acid (0.02 N) while stirring magnetically. The resulting solution was transparent and had a collagen concentration of 3.8 mg/mL. Following that, a volume of 1.8 mL of phosphate-buffered saline (PBS) with a pH of 7.4, containing LEO-NE at a concentration of 1% by weight, was introduced into the collagen solution. The pH of the solution was then brought to 7.4 by adding a solution of 0.5 M NaOH. The collagen solution was prepared and neutralized on ice. To induce collagen fibrillation and hydrogel formation, the solution was subjected to incubation at a temperature of 37°C for a duration of 2 hours (17).

Hydrogel characterization: gelation time measurement. The gelation time was determined by conducting a vial inversion test, following the methodology outlined by Gupta et al. In this procedure, the hydrogel solution was not subjected to vial inversion to determine the gelation time. The duration of collagen transmission in the sol-gel was measured by rotating the vial every 10 seconds. A gelation time was measured when the collagen solution did not remain buoyant after the vial was returned. Each sample was recorded with an average value of three duplicates (18).

Hydrolytic degradation. The lyophilized hydrogel samples were precisely weighed and thereafter submerged in 10 mL of PBS at various time intervals for a maximum duration of 21 days, with the solution being replaced every 2 days. Following each time point, the samples were extracted from PBS and rinsed with deionized water. Subsequently, they were subjected to freezing, lyophilization, and weighing. The weight loss % (degradation) was determined by comparing the dry mass of samples before and after immersion, using the equation: where W_1 represents the initial dry weight of lyophilized hydrogel, and W_2 represents the dry weight of lyophilized hydrogel after each time interval. Three specimens from each hydrogel group were assessed, and the mean value was documented (19).

$$\text{Weight loss\%} = (w_1 - w_2)/w_1 \times 100$$

Swelling ratio. The swelling properties were assigned to evaluate the hydrophilic scaffolds. In summary, the lyophilized samples (W_d) were placed in PBS (pH 7.4) and kept at a temperature of 37°C for a period of time. After 30 minutes, the weight of the samples when they were wet (W_w) was measured. The percentage of swelling was determined by applying the following equation: where Wd represents the original dry weight and W_w represents the wet weight of the samples. The equation was used to get the average of three values for each sample (17).

$$\text{Swelling ratio \%} = \frac{w_w - wd}{w_d} \times 100$$

Isolation, identification, and antimicrobial susceptibility testing. With the aim of isolating MDR bacteria, wound swabs were collected from patients experiencing burn injuries. with signs of infection at Zare Hospital. The swab specimens were cultured on Tryptic Soy Broth (TSB) to initiate growth, and the initial isolation was performed on blood agar. The conventional techniques were employed to identify *P. aeruginosa*, which encompassed gram staining, analysis of colony shape, growth at 44°C, catalase, oxidase, and Triple Sugar Iron (TSI) fermentation tests. The disk diffusion method was implemented following the standards suggested by the Clinical and Laboratory Standards Institute (CLSI) to ascertain the antimicrobial susceptibility. The antibiotic disks (Mast Group Co, UK) used in this study included cefepime (30 µg), piperacillin-tazobactam (100/10 µg), meropenem (10 µg), imipenem (10 µg), aztreonam (30 µg), piperacilin (100 µg), Gentamicin (10 µg), Tobramycin (10 µg), Amikacin (30 µg), Ceftazidime (30 µg) and ciprofloxacin (5 µg). An isolate that is resistant to at least three classes of antibacterial agents is classified as MDR (20).

Determination of minimum inhibitory concentration (MIC) and minimum bactericidal concentration (MBC). The MIC values were calculated using the micro-broth dilution method recommended by the CLSI. This approach involved using Mueller-Hinton broth (MHB) medium and overnight bacterial cultures with a concentration of 5×10^5 colony-forming units per milliliter (CFU/mL). Various quantities of NEs were added to 1 mL tubes containing MHB and standard bacterial suspensions. The mixtures were then incubated at 37°C for 18 hours. The MIC value was defined as the concentration of the first tube where no visible signs of growth were observed. The controls consisted of MHB plus NE and MHB plus solvent. The MBC value was determined by measuring the concentration of NE that effectively suppressed bacterial growth, resulting in the absence of colonies on the Mueller-Hinton Agar plate (21). This test was done with three repetitions.

Animals. The animals remained in a controlled environment at a temperature range of 22-25°C. They were exposed to a 12-hour cycle of light and darkness and had free access to water and food. The rats equipment was sterilized using an autoclave. In addition, the cages were sterilized using a 10% povidone-iodine solution in order to enhance the accuracy of bacterial assessments. The experimental techniques were authorized by the ethical committee of Mazandaran University of Medical Sciences in compliance with the requirements for the welfare and utilization of laboratory animals. Animals were anesthetized with ketamine (80 mg/kg, i.p.) and xylazine (10 mg/kg, i.p.). After shaving the back hair and cleaning the skin with 70% ethanol, a full-thickness circular skin wound (diameter 10 mm) was created in the midline of the back of each animal by a cylindrical iron rod previously placed on a flame. Burns were performed by induction of the second-degree burn model (22). The rats were then randomly divided into four groups of five rats each: negative control (serum physiology), positive control (silver sulfadiazine cream), collagen hydrogel, and collagen hydrogel-containing LEO-NE. After the burn site had cooled, the wounds were infected with 100 microliters of *P. aeruginosa* 0.5 McFarland. A bacterial culture was done to be sure the wound was infected. For the control groups, the treatment was done every day, and for the hydrogels, the treatment was done all at once (23).

Wound closure measurement. Wound closure measures were taken on days 4, 11, and 18. The mean wound size was measured using a caliper. The percentage of wound closure was determined by calculating the ratio of the difference between the primary wound area (A_0) and the area of the wound at the time of measurement (A_t) to the original wound area (A_0) (24).

$$\text{Percentage of wound closure} = (A_0 - A_t)/A_0 \times 100$$

Histological analysis. On the 4th, 11th, and 18th days, the skin burn site biopsy samples were pre-

served in a formalin 10% solution and made ready for pathology tests. The sections (4 μm) underwent deparaffinization and rehydration for hematoxylin and eosin (H&E) staining. After staining, the important parameters in the burn process of wound healing were examined, and the degree of epithelialization, fibroblast, proliferation, angiogenesis, formation of collagen fibers, and presence of inflammatory cells were evaluated. Trichrome staining of tissue samples was done to check the degree of collagen deposition (25). The pathologist examined the skin tissues and assessed them using Abramov's grading system. Each section was assigned a score between 0 and 3. Scores ranged from 0 to 3, including 0 = no attendance, 1 = low, 2 = moderate, and 3 = high (26).

Statistical analysis. The percentage of wound closure was quantified as the average value ± the standard deviation. The groups were compared using the Kruskal-Wallis test, whereas the comparison of two groups was conducted using the Mann-Whitney test. P value <0.05 was considered significant. The analyses were conducted using SPSS 21.0.

Ethical approval. This study was confirmed by the Ethics committee of Aja university of medical sciences. Confirmation code: IR.AJAUMS.REC.1401.212(2023.02.19).

RESULTS

Composition of LEO. The GC/MS spectrum results from this research, out of 101 compounds in LEO, there were eight major compounds with an amount greater than 4%, which is equivalent to 64.77% of the whole compositions, all of which are monoterpenes (Table 1). As can be seen in the Table, these eight items are in order of abundance: 1,8-cineole (22.29%), Linalool (11.22%), Camphor (7.88%), β-pinene (5.78%), α-terpineol (4.85%), α-Pinene (4.53%), Terpinen-4-ol (4.19%), and Borneol (4.03%).

Characterization of LEO-NE. The particle size analysis of all formulations was done with Zetasizer. Fig. 1b shows the zeta potential of LEO-NE, which measured -9.82 ± 6 mV. The average zeta potential of LEO-NEs was -16.18 ± 1.03 mV . The mean ± SD diameter of LEO-NE was found to be 105.6 ± 7.875 nm, with a PDI of 0.331 ± 0.055. The entirety of the system exhibits a preference for a negative charge, which promotes heightened stability through the repellent effect of like charges. Fig. 1a presents data on the particle size and PDI of an individual formulation. The findings have verified that the NPs exhibit a nanoscale dimension with a distinct and singular peak, consequently supporting the uniformity of the NPs with a narrow spectrum of particle size distribution. The assessment of the stability of NE relies on the analysis of droplet size and size distribution, which can serve as indicators of drug release and absorption within these formulations.

Table 1. Main chemical substances (more than 4%) of *Lavandula officinalis* essential oil

	Compounds	RI[a]	GC region (%)
1	α-Pinene	932	4.53
2	β-pinene	974	5.78
3	1,8-cineole	1026	22.29
4	Linalool	1095	11.22
5	Campher	1141	7.88
6	Borneol	1165	4.03
7	Terpinen-4-ol	1174	4.19
8	α-terpineol	1186	4.85
9	Other compounds		32.23
Total			64.77

RI[a]: Retention indices on DB-5 column.

Hydrogel characterization: gelation time. Collagen hydrogels were created by altering the pH and temperature of solutions containing collagen and collagen/LEO-NE hydrogels. The fibrillation and gelation of collagen take place when the pH and temperature of the acidic collagen solution approach 7.4 and 37°C, respectively. Alterations in the composition of the hydrogel solution can potentially influence the gelation time of collagen. In order to assess the impact of including LEO-NE on the gelation time of collagen hydrogel, we conducted a vial inversion test. The gelation periods of collagen and collagen/LEO-NE hydrogel solutions are displayed in Fig. 2. According to the figure, the inclusion of LEO-NE in the collagen solution resulted in a longer time for the gel to form. The collagen solution lacking LEO-NE did form a gel within 30 ± 1 seconds, but the gelation time for Col/LEO-NE was 57 ± 24 seconds. The late gelation of the collagen/LEO-NE solution may have been caused by potential interactions between collagen and LEO-NE.

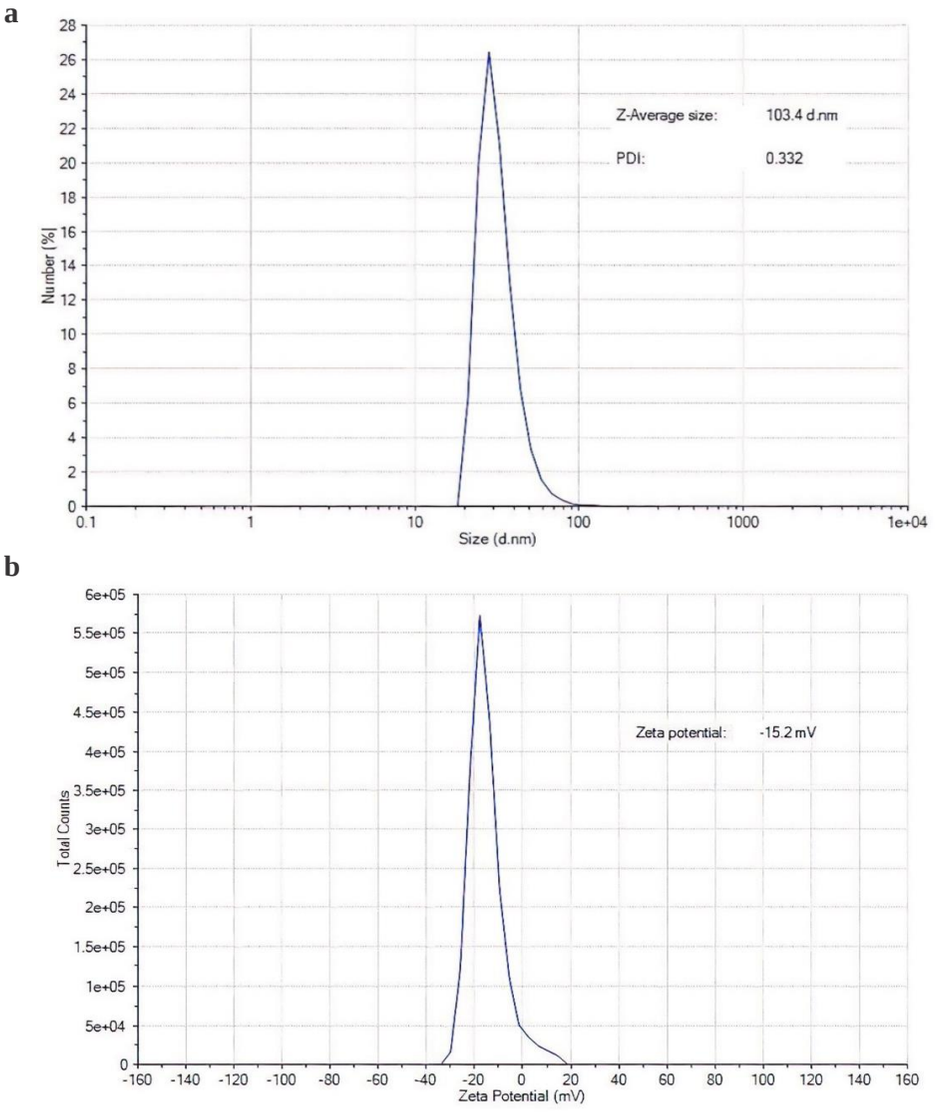

Fig. 1. The Z-average size, poly-dispersity index (PDI) (1a), and Zeta potential (1b) of a specific LEO-NE
a. The Z-average size and poly-dispersity index (PDI) L EO-NE
b. Zeta potential of a specific L EO-NE

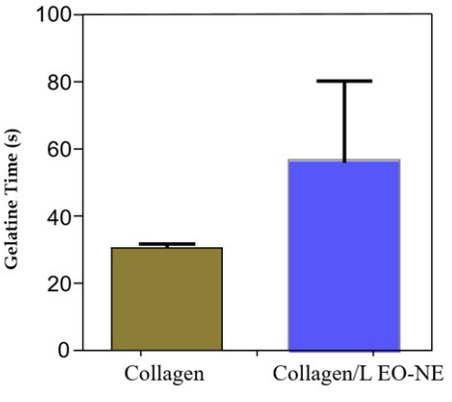

Fig. 2. Time needed for collagen and collagen/LEO-NE to gel.

Hydrolytic degradation. The weight loss of the hydrogel was examined by measuring the weight of the immersed scaffolds in PBS at various time intervals, up to a maximum of 21 days. The proportion of residual weight was determined by comparing the dry mass of the samples before and after immersion. The proportion of weight reduction for each scaffold is displayed in Fig. 3. Based on the figure, the pure collagen scaffold exhibited more weight loss at all time intervals compared to collagen/LEO-NE. After a duration of 1 week, the weight loss percentage for pure collagen was approximately 75%, whereas for collagen/LEO-NE it was around 43%. The pure collagen scaffold

saw a weight loss of approximately 79% after 21 days, whereas the collagen/LEO-NE composite exhibited a weight reduction of around 62% during the same period. The presence of stronger bonding contacts between collagen and LEO-NE may result in a reduced erosion rate of the collagen/LEO-NE composite.

Swelling ratio. Fig. 4 shows the swelling ratio of pure collagen and collagen/LEO-NE scaffolds after immersing in PBS (pH 7.4) for 30 minutes. The swelling ratio of pure collagen was approximately 5.6 ± 0.24 g. The addition of LEO-NE to collagen hydrogels led to an increase in the swelling ratio. As the content of LEO-NE increased, the swelling ratios of the hydrogels also increased. The swelling ratio for collagen/LEO-NE was 20 g ± 4 g. The structure and hydrophilic properties of the scaffold material influence the amount of swelling.

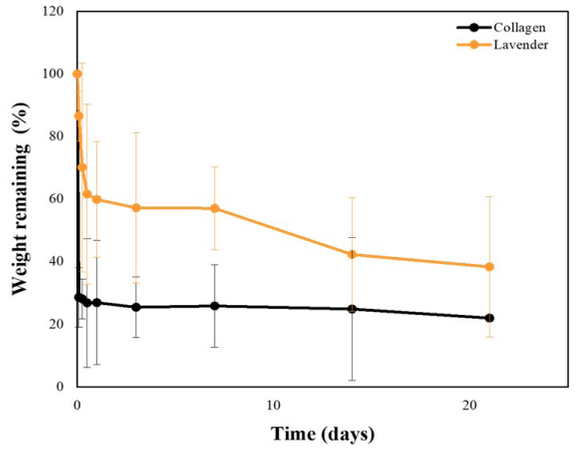

Fig. 3. Weight loss of scaffolds in PBS (pH 7.4) at various time intervals.

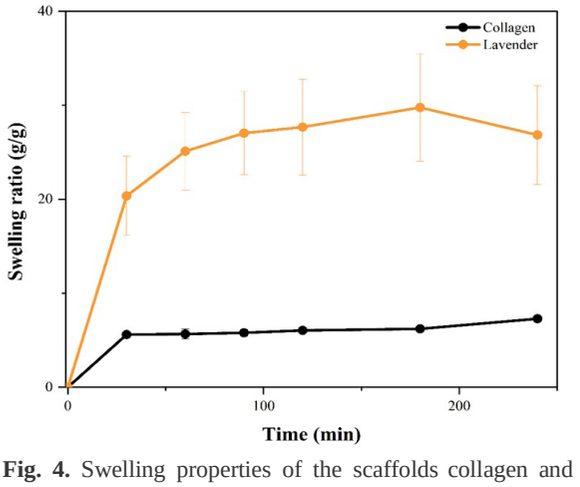

Fig. 4. Swelling properties of the scaffolds collagen and LEO-NE after immersing them in PBS (pH 7.4) for 30 minutes.

Antibiotic resistance. *P. aeruginosa* was subjected to antimicrobial susceptibility testing to evaluate the resistance pattern (Table 2), and MDR was determined based on the results, which was resistant to all antibiotics except cefepime and piperacillin-tazobactam and showed intermediate resistance to imipenem.

Determination of minimum inhibitory concentration (MIC) and minimum bactericidal concentration (MBC). As indicated in the Table 3, the MIC of LEO-NE against *P. aeruginosa* and *S. aureus* were 156 and 156 µg/mL, and the MBC were 312 and 2500 µg/mL, in the order mentioned. In addition, according to the MIC and MBC of the bacteria, LEO-NE had a bacteriostatic effect on both bacteria, but it had a bactericidal effect on *P. aeruginosa* and a bacteriostatic effect on *S. aureus.*

Wound closure. Fig. 5 shows the comparative graph of wound closure percentage among the study groups on the 4th, 11th, and 18th days. Table 4 presents the average percentage of wound closure for the four groups. The Kruskal-Wallis test revealed a significant difference between the groups in terms of the percentage of wound closure (P-value <0.05).

Upon pairwise analysis of the groups using the Mann-Whitney U test, a notable distinction was seen between the second experimental group and the others (collagen hydrogel containing LEO-NE) and the positive control (silver sulfadiazine ointment) on the fourth day. There was a notable disparity between the second experimental group and the negative control group on the 4th day (P-value = 0.032) and 11th day (P-value = 0.032). Also, according to the Mann-Whitney test, There was a notable disparity between the negative control group (collagen hydrogel) and the first and second trial group (LEO-NE) on the day (P-value = 0.032). On the 18th day, due to the decrease in the number of rats due to death, the results of paired group analysis and the Mann-Whitney test did not show significant differences (P-value >0.05).

Histological analysis. In pathology studies, effective parameters for burn wound healing, including the formation of epithelium, fibroblasts, proliferation, angiogenesis, collagen fibers, and inflammatory cells, were evaluated. The above criteria were scored by H&E

Table 2. Result of antibiotic resistance of *P. aeruginosa*

Cefepime	Piperacillin-tazobactam	Meropenem	Imipenem	Aztreonam	Piperacilin
S	S	R	I	R	R
Gentamicin	**Tobramycin**	**Amikacin**	**Ceftazidime**	**Ciprofloxacin**	
R	R	R	R	R	

Abbreviation R: resistance, S: susceptibility, I: intermediate

Table 3. MIC and MBC of 1% LEO-NE in micrograms per milliliter

	MIC (µg/mL)	MBC (µg/mL)
P. aeruginosa	156	312
S. aureus	156	2500

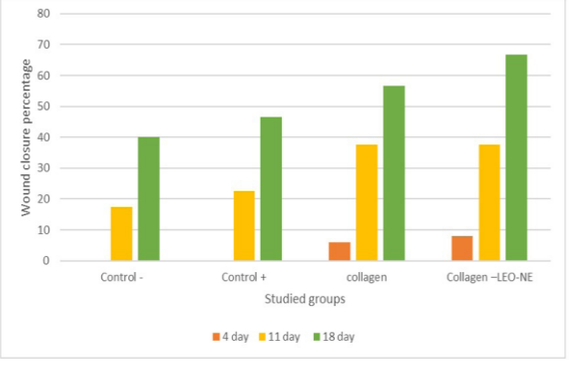

Fig. 5. The graph of the average percentage of wound closure in the groups on days 4, 11 and 18

and trichrome staining with light microscopy. Under a microscope, the quantity of neutrophils revealed acute inflammation; chronic inflammation was measured by counting the numeral of lymphocytes and macrophages. The number of vessels that formed in the inflamed area was the method used to assess angiogenesis, and fibrosis was evaluated by the number of underlying fibroblasts. The results are shown based on the average score and as a graph in Fig. 6. Masson's trichrome staining was performed on day 18 to examine collagen deposition. The blue collagen bands in trichrome staining represent the deposition of collagen (Fig. 7). The negative control (serum) group has only mild deposition of collagen; the positive control (silver sulfadiazine) group has haphazardly arranged collagen bundles; the collagen group is less organized; and the collagen/LEO-NE group shows well-organized parallel bundles. In preliminary investigations (day 4), the rate of acute inflammation, edema, and fibrin deposition was high in all groups, but the treatment with LEO-NE and silver sulfadiazine groups had anti-inflammatory effects. Day 11: Chronic inflammation was seen in negative control (serum) and, to a lesser extent, in the positive control (silver sulfadiazine), while it was less common in the hydrogel collagen and hydrogel collagen-containing LEO-NE groups. Angiogenesis and fibroplasia were seen in the LEO-NE treatment group at a moderate level. Both treatment groups with hydrogel scaffolds had a moderate amount of collagen deposition. Epithelization was seen in any group due to high inflammation, but only in the hydrogel/LEO-NE group. In the positive control group, mild angiogenesis was seen with fibroblastic proliferation, and in the experimental group, moderate vascularization and fibroblastic proliferation were seen. Day 18: In the negative control group, there was chronic inflammation, mild chronic inflammation, and fibrosis in the positive control group, and modest collagen deposition in the hydrogel groups (Fig. 8).

DISCUSSION

In this study, the wound healing effects of collagen hydrogel scaffold and collagen hydrogel/LEO-NE on burn wounds (flame) infected with *P. aeruginosa* MDR in an animal model (rat) were investigated by examining pathological parameters. We have successfully produced a novel hydrogel formulation based on collagen, loaded with LEO-NE, to facilitate the recovery of infected burn wounds and prevent the emergence of pathogenic infections. Evaluation of EO composition showed main monoterpenes similar to previous studies (27). The results confirmed the beneficial effects of hydrogel and LEO-NE containing hydrogel on wound healing. Hydrogel collagen/LEO-NE was able to reduce inflammation, increase collagen production, and cause the wound to close faster, which is probably due to LEO's antibacterial and antioxidant properties. Of course, in this study

Table 4. Determination of significance between four groups with the Kruskal-Wallis test

Day	Control -	Control +	Collagen	Collagen –LEO-NE	P value
	Mean ± Std.Division				
4	0.00 ± 0.00	0.00 ± 0.00	6.00 ± 5.47	8.00 ± 4.47	0.014
11	17.50 ± 5.00	22.5 ± 9.57	37.50 ± 5.00	37.50 ± 5.00	0.011
18	40.00 ± 10.00	46.66 ± 5.77	56.66 ± 5.77	66.67 ± 5/77	0.034

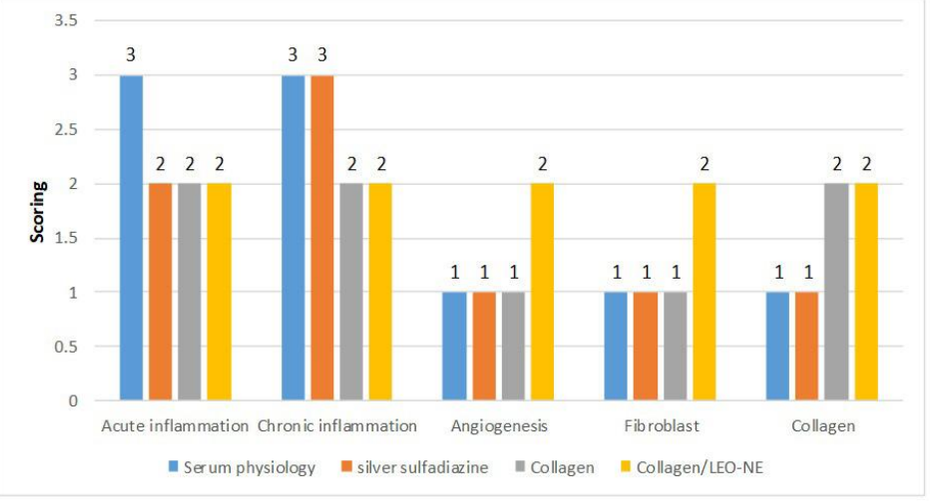

Fig. 6. Average pathology scores of treatment groups. Scores ranged from 0 to 3, including 0=no attendance, 1=low, 2=moderate, and 3=high. (Axis x, parameters studied in pathology) (Axis y, scoring system)

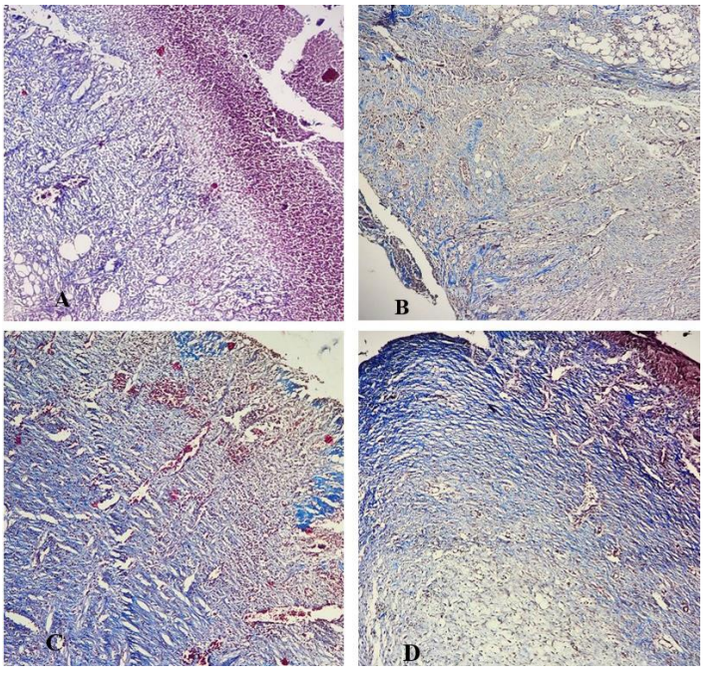

Fig. 7. Masson's trichrome stain in day 18, (A) negative control (serum) group with only mild deposition of collagen, (B) positive control (Silver sulfadiazine) group with haphazard arranged collagen bundles, (C) Collagen group with less organized blue stained, (D) Clollagen/LEO-NE showing well organized parallel bundles of collagen that stained blue (X400).

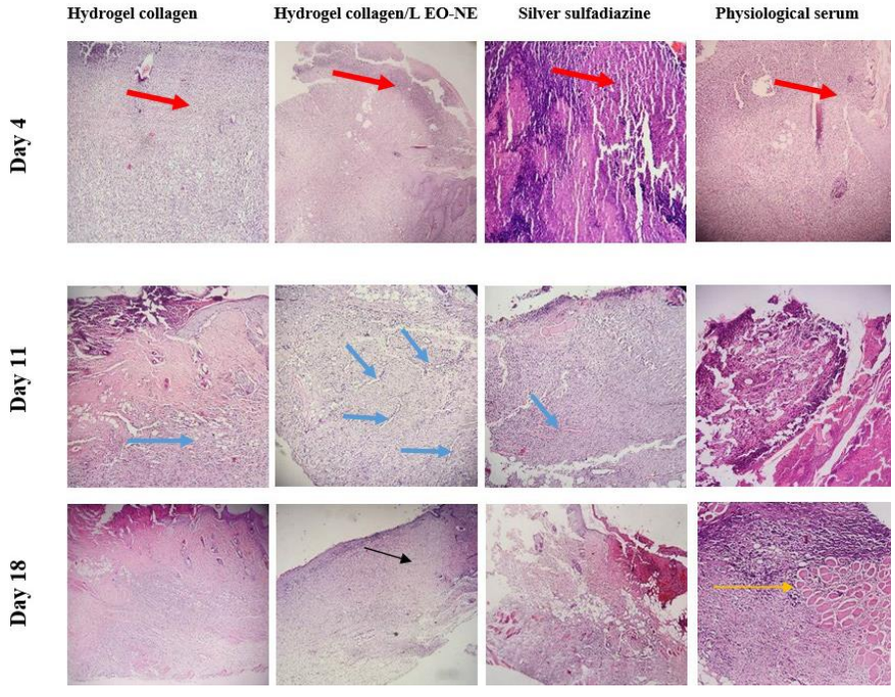

Fig. 8. Histological assessment of tissues stained with Haematoxylin and Eosinof treatment groups in the 4th, 11th, and 18th days (200X). The red arrow is acute inflammation. Blue arrow is angiogenesis more degree in treatment group. The yellow arrow indicates persistent chronic inflammation.The black arrow shows the epithelialization in the hydrogel collagen/LEO-NE group (100X).

examined the impact of LEO-NE for the first time on *P. aeruginosa*, which indicates its antimicrobial effects. In line with this study, Fadel et al. (2023) examined the antibacterial properties of LEO-NE on *Proteus mirabilis* (28). The study conducted by Derya Demir et al. in 2023 demonstrated the efficacy of *lavandula* in enhancing wound healing in individuals with diabetes. Additionally, the findings of this study demonstrated that LEO augmented the synthesis of collagen, epithelialization, and fibroblasts, aligning with the outcomes of the current investigation (29). In another study, *lavandula* was employed for its antibacterial and anti-inflammatory properties in a hydrogel formulation aimed at treating infected wounds. The results demonstrated highly effective antimicrobial activity against *S. aureus* and *C. albicans.* Also, the research showed that the hydrogel containing *lavandula* had a heightened antioxidant impact in comparison to the scaffold without oil. This enhanced antioxidant effect has the potential to expedite the wound healing process. Derya Demir et al. conducted a study in 2023 that demonstrated the efficacy of *lavandula* in enhancing wound healing in individuals with diabetes. Also, the results of this investigation show that LEO enhanced the synthesis of collagen, epithelialization, and fibroblasts, aligning with the results of the current study (30).

Wounds are a common medical problem that can arise from various skin injuries, such as surgical interventions, pressure sores, burns, and diabetic ulcers. Consequently, medical practice frequently utilizes them. However, even though wounds are common, there are only a few officially recognized therapies available for the process of healing wounds. Present guidelines for fundamental wound care involve commencing antibiotic treatment exhibiting clinical infection, removing necrotic tissue or pollutants from wounds through debridement, and applying dressings that sustain a moist environment (14). Bacterial resistance to antibiotics has significantly surged, hence restricting their therapeutic efficacy. Furthermore, there has been a notable decline in the efficacy of recently developed antibiotics and chemotherapeutics. The hydrogel's antibacterial activity could be enhanced by including plant EOs with antibacterial properties. EOs primarily exert their antibacterial effects by interacting with the cytoplasmic membrane. This engagement causes instability

in the membrane and increases its permeability (31-33). The process of healing a skin wound is an intricate molecular and cellular process that consists of four active phases: coagulation, inflammation, proliferation, and regeneration. These phases synergistically collaborate to reinstate the initial structure and functionality of the impaired tissue (14). Collagen, an essential component of the extracellular matrix, has a vital function in the process of wound healing. This mechanism depends on the regulated synthesis and buildup of collagen fibers. Research indicates that type III collagen is more abundant in the early phases of wound healing, while type I collagen replaces it in the later stages. These stages collaborate to reinstate the initial structure and functionality of the impaired tissue (34). LEO has been shown to accelerate wound contraction and exhibit antibacterial properties, making it a promising candidate for topical therapy with dual benefits (32, 35).

In this study, several NE formulations were prepared (data were not shown), and the most suitable NE based on particle size, pdi, and zeta potential was selected for hydrogel preparation because the electric potential, known as zeta potential, emerges from the existence of a charge on a particle's surface, and its polarity is linked to the chemical characteristics of the particles, with the potential being either positive or negative. The zeta potential exhibited by a given formulation can potentially function as an indicator of its physical stability (36). The small dimensions of NE droplets lead to a higher specific surface area, which in turn facilitates enhanced interaction with the bacterial cell membrane. In addition, the process of nano-emulsification effectively inhibits the oxidation and evaporation of the EO contents (37). Potential interactions between collagen and LEO-NE may have caused the late gelation of the collagen/LEO-NE solution. Fig. 4 in this work demonstrates the percentage swelling of optimum LEO-NE-hydrogel, which can be divided into two distinct phases: the growing time and a period of relative stability. Over a 24-hour period, the swelling percentages of LEO-NE-hydrogel increased significantly. The moisture present in the hydrogels influenced this increase, demonstrating their strong hydrophilicity. The hydrogels' moisture absorption capacity remained unchanged after 72 hours, indicating that they had reached a state of saturation. Hydrogels and nanocomposites' swelling capacity and structural stability are critical for their biological applications (38). The swelling behavior of optimal hydrogels was evaluated based on their moisture absorption values. The polymer can swell due to interactions between collagen chains and water molecules. The degree of swelling on a scaffold is determined by its composition and hydrophilic characteristics. If these materials can retain the three-dimensional architecture of the hydrogel, it will enhance its capacity to absorb and retain water. Because collagen and LEO-NE have stronger bonding contacts, the collagen/LEO-NE composite may not wear away as quickly. Since most herbal compounds are safe, we recommend studying other EOs and extracts mixed into hydrogel scaffolds to see how they work on their own and together to help wounds heal, whether they are infected or not due to the safety of most herbal compounds, it is suggested to investigate other EOs and extracts loaded in hydrogel scaffolds to investigate the healing of infected or non-infectious wounds, both individually and synergistically.

One of the limitations of the study was that microbial culture was not performed on the wound samples after treatment, which is why it is recommended for other researchers to assay the outcome of LEO-NE on the number of bacteria in addition to wound healing through CFU/mL. The sample size (number of rats) was small in the studied groups. Also, in this study, wound healing infected with *P. aeruginosa* drug-resistant Gram-negative bacteria was investigated. It is recommended that other researchers in their studies, while removing the limitations, examine this compound (LEO-NE) and other herbal compounds and their effect on the treatment of infected burn wounds with drug-resistant bacteria, such as *S. aureus,* is a process of healing.

CONCLUSION

This study used an animal model to test a collagen hydrogel combined with LEO-NE to investigate its effects on burn wounds infected with *P. aeruginosa* MDR. Based on H&E stain, interpretation of pathology resaults, Masson's trichrome stain, and wound diameter contraction, treatment groups containing collagen reduce inflammation (acute and chronic), increase collagen production and angiogenesis, and also make the procedure of wound healing faster. Collagen production was higher in the studied groups. LEO-NE showed good antibacterial effects against antibiotic-resistant *P. aeruginosa* because

bacterial resistance mechanisms against LEO-NE are ineffective, unlike common antibiotics. Among the several treatment groups, the LEO-NE hydrogel demonstrates the highest potential as a wound dressing. The results of the study can provide an important perspective on the treatment of wounds with alternative drugs to antibiotics.

ACKNOWLEDGEMENTS

The authors express gratitude to the research council of Aja University of Medical Sciences.

REFERENCES

1. Xiong Y, Xu Y, Zhou F, Hu Y, Zhao J, Liu Z, et al. Bio-functional hydrogel with antibacterial and anti-inflammatory dual properties to combat with burn wound infection. *Bioeng Transl Med* 2022; 8(1): e10373.
2. Zhu C, Zhao J, Kempe K, Wilson P, Wang J, Velkov T, et al. A Hydrogel-Based Localized release of colistin for antimicrobial treatment of burn wound infection. *Macromol Biosci* 2017; 17: 10.1002/mabi.201600320.
3. Moeini A, Pedram P, Makvandi P, Malinconico M, Gomez d'Ayala G. Wound healing and antimicrobial effect of active secondary metabolites in chitosan-based wound dressings: A review. *Carbohydr Polym* 2020; 233: 115839.
4. Boateng J, Catanzano O. Advanced therapeutic dressings for effective wound Healing--A review. *J Pharm Sci* 2015; 104: 3653-3680.
5. Sahana TG, Rekha PD. Biopolymers: Applications in wound healing and skin tissue engineering. *Mol Biol Rep* 2018; 45: 2857-2867.
6. Samadi A, Azandeh S, Orazizadeh M, Bayati V, Rafienia M, Karami MA. Fabrication and characterization of Glycerol/Chitosan/Polyvinyl Alcohol-Based transparent hydrogel films loaded with silver nanoparticles for antibacterial wound dressing applications. *Adv Biomed Res* 2021; 10: 4.
7. Abbasi K, Tavakolizadeh S, Hadi A, Hosseini M, Soufdoost RS, Heboyan A, et al. The wound healing effect of collagen/adipose-derived stem cells (ADSCs) hydrogel: *In vivo* study. *Vet Med Sci* 2023; 9: 282-289.
8. Ansari MN, Soliman GA, Rehman NU, Anwer MK. Crisaborole loaded nanoemulsion based chitosan gel: formulation, physicochemical characterization and wound healing studies. *Gels* 2022; 8: 318.
9. Dolgachev VA, Ciotti S, Liechty E, Levi B, Wang SC, Baker JR, et al. Dermal nanoemulsion treatment reduces burn wound conversion and improves skin healing in a Porcine model of thermal burn injury. *J Burn Care Res* 2021; 42: 1232-1242.
10. Hamdan S, Pastar I, Drakulich S, Dikici E, Tomic-Canic M, Deo S, et al. Nanotechnology-driven therapeutic interventions in wound healing: potential uses and applications. *ACS Cent Sci* 2017; 3: 163-175.
11. Zarrintaj P, Moghaddam AS, Manouchehri S, Atoufi Z, Amiri A, Amirkhani MA, et al. Can regenerative medicine and nanotechnology combine to heal wounds? The search for the ideal wound dressing. *Nanomedicine (Lond)* 2017; 12: 2403-2422.
12. Kačániová M, Vukic M, Vukovic NL, Čmiková N, Verešová A, Schwarzová M, et al. An in-depth study on the chemical composition and biological effects of *Pelargonium graveolens* essential oil. *Foods* 2023; 13: 33.
13. Mele E. Electrospinning of essential oils. *Polymers (Basel)* 2020; 12: 908.
14. Samuelson R, Lobl M, Higgins S, Clarey D, Wysong A. The effects of lavender essential oil on wound healing: A review of the Current evidence. *J Altern Complement Med* 2020; 26: 680-690.
15. Li W, Lan Y, Guo R, Zhang Y, Xue W, Zhang Y. *In vitro* and *in vivo* evaluation of a novel collagen/cellulose nanocrystals scaffold for achieving the sustained release of basic fibroblast growth factor. *J Biomater Appl* 2015; 29: 882-893.
16. Morteza-Semnani K, Saeedi M, Akbari J, Eghbali M, Babaei A, Hashemi SMH, et al. Development of a novel nanoemulgel formulation containing cumin essential oil as skin permeation enhancer. *Drug Deliv Transl Res* 2022; 12: 1455-1465.
17. Gatabi ZR, Saeedi M, Morteza-Semnani K, Rahimnia SM, Yazdian-Robati R, Hashemi SMH. Green preparation, characterization, evaluation of anti-melanogenesis effect and *in vitro/in vivo* safety profile of kojic acid hydrogel as skin lightener formulation. *J Biomater Sci Polym Ed* 2022; 33: 2270-2291.
18. Gupta D, Tator CH, Shoichet MS. Fast-gelling injectable blend of hyaluronan and methylcellulose for intrathecal, localized delivery to the injured spinal cord. *Biomaterials* 2006; 27: 2370-2379.
19. Shahrezaee M, Salehi M, Keshtkari S, Oryan A, Kamali A, Shekarchi B. *In vitro* and *in vivo* investigation of PLA/PCL scaffold coated with metformin-loaded gelatin nanocarriers in regeneration of critical-sized bone defects. *Nanomedicine* 2018; 14: 2061-2073.
20. Karami P, Mohajeri P, Yousefi Mashouf R, Karami M, Yaghoobi MH, Dastan D, et al. Molecular characterization of clinical and environmental *Pseudomonas aeruginosa* isolated in a burn center. *Saudi J Biol Sci* 2019; 26: 1731-1736.
21. Chaieb K, Kouidhi B, Jrah H, Mahdouani K, Bakhrouf A. Antibacterial activity of Thymoquinone, an active

principle of *Nigella sativa* and its potency to prevent bacterial biofilm formation. *BMC Complement Altern Med* 2011; 11: 29.
22. Said A, Naeem N, Siraj S, Khan T, Javed A, Rasheed HM, et al. Mechanisms underlying the wound healing and tissue regeneration properties of *Chenopodium album*. *3 Biotech* 2020; 10: 452.
23. Kambouris AR, Brammer JA, Roussey H, Chen C, Cross AS. A combination of burn wound injury and *Pseudomonas* infection elicits unique gene expression that enhances bacterial pathogenicity. *mBio* 2023; 14(6): e0245423.
24. Putra A, Ibrahim S, Muhar AM, Kuntardjo N, Dirja BT, Pasongka Z, et al. Topical gel of mesenchymal stem cells-conditioned medium under TNF-α precondition accelerates wound closure healing in full-thickness skin defect animal model. *J Med Life* 2022; 15: 214-221.
25. Khalid A, Khan R, Ul-Islam M, Khan T, Wahid F. Bacterial cellulose-zinc oxide nanocomposites as a novel dressing system for burn wounds. Bacterial cellulose-zinc oxide nanocomposites as a novel dressing system for burn wounds. *Carbohydr Polym* 2017; 164: 214-221.
26. Abramov Y, Golden B, Sullivan M, Botros SM, Miller JJ, Alshahrour A, et al. Histologic characterization of vaginal vs. abdominal surgical wound healing in a rabbit model. Histologic characterization of vaginal vs. abdominal surgical wound healing in a rabbit model. *Wound Repair Regen* 2007; 15: 80-86.
27. Adal AM, Demissie ZA, Mahmoud SS. Identification, validation and cross-species transferability of novel Lavandula EST-SSRs. *Planta* 2015; 241: 987-1004.
28. Fadel BA, Elwakil BH, Fawzy EE, Shaaban MM, Olama ZA. Nanoemulsion of lavandula angustifolia essential Oil/Gold Nanoparticles: Antibacterial effect against Multidrug-Resistant Wound-Causing bacteria. *Molecules* 2023; 28: 6988.
29. Demir D, Toygar I, Soylu E, Aksu AT, Türeyen A, Yıldırım I, et al. The effect of lavandula stoechas on wound healing in an experimental diabetes model. The effect of lavandula stoechas on wound healing in an experimental diabetes model. *Cureus* 2023; 15(9): e45001.
30. Rusu AG, Niță LE, Roșca I, Croitoriu A, Ghilan A, Mititelu-Tarțău L, et al. Alginate-based hydrogels enriched with lavender essential oil: evaluation of physicochemical properties, antimicrobial activity, and *in vivo* biocompatibility. *Pharmaceutics* 2023; 15: 2608.
31. Chouhan S, Sharma K, Guleria S. Antimicrobial activity of some essential Oils-Present status and future perspectives. *Medicines (Basel)* 2017; 4: 58.
32. Predoi D, Iconaru SL, Buton N, Badea ML, Marutescu L. Antimicrobial activity of new materials based on lavender and basil essential oils and hydroxyapatite. *Nanomaterials (Basel)* 2018; 8: 291.
33. Keyhanian A, Mohammadimehr M, Nojoomi F, Naghoosi H, Khomartash MS, Chamanara M. Inhibition of bacterial adhesion and anti-biofilm effects of *Bacillus cereus* and *Serratia nematodiphila* biosurfactants against *Staphylococcus aureus* and *Pseudomonas aeruginosa*. *Iran J Microbiol* 2023; 15: 425-432.
34. Mathew-Steiner SS, Roy S, Sen CK. Collagen in Wound Healing. *Bioengineering (Basel)* 2021; 8: 63.
35. Vasireddy L, Bingle LEH, Davies MS. Antimicrobial activity of essential oils against multidrug-resistant clinical isolates of the Burkholderia cepacia complex. *PLoS One* 2018; 13(8): e0201835.
36. Chaiyana W, Inthorn J, Somwongin S, Anantaworasakul P, Sopharadee S, Yanpanya P, et al. The fatty acid compositions, irritation properties, and potential applications of teleogryllus mitratus oil in nanoemulsion development. *Nanomaterials (Basel)* 2024; 14: 184.
37. Fattahi R, Ghanbarzadeh B, Dehghannya J, Hosseini M, Falcone PM. The effect of Macro and Nano-emulsions of cinnamon essential oil on the properties of edible active films. *Food Sci Nutr* 2020; 8: 6568-6579.
38. Masood N, Ahmed R, Tariq M, Ahmed Z, Masoud MS, Ali I, et al. Silver nanoparticle impregnated chitosan-PEG hydrogel enhances wound healing in diabetes induced rabbits. *Int J Pharm* 2019; 559: 23-36.